MOUNTAIN-PLAINS CONSORTIUM

MPC 24-532 | C. Pantelides and D. Briggs

NUMERICAL SIMULATION OF STRENGTHENING OF BRIDGE DECKS BUILT WITH PARTIAL DEPTH PRECAST CONCRETE DECK PANELS

MOUNTAIN-PLAINS CONSORTIUM REGION 8

A University Transportation Center sponsored by the U.S. Department of Transportation serving the Mountain-Plains Region. Consortium members:

Colorado State University
North Dakota State University
South Dakota State University
University of Colorado Denver
University of Denver
University of Utah
Utah State University
University of Wyoming

Technical Report Documentation Page

1. Report No.	2. Government Accession No.	3. Recipient's Catalog No.
MPC-670		

4. Title and Subtitle	5. Report Date
Numerical Simulation of Strengthening of Bridge Decks Built with Partial Depth Precast Concrete Deck Panels	July 2024
	6. Performing Organization Code

7. Author(s)	8. Performing Organization Report No.
Chris P. Pantelides Dylan Briggs	MPC 24-532

9. Performing Organization Name and Address	10. Work Unit No. (TRAIS)
Department of Civil and Environmental Engineering The University of Utah 110 Central Campus Drive, Room 2000 Salt Lake City, UT 84112	11. Contract or Grant No.

12. Sponsoring Agency Name and Address	13. Type of Report and Period Covered
Mountain-Plains Consortium North Dakota State University PO Box 6050, Fargo, ND 58108	Final Report
	14. Sponsoring Agency Code

15. Supplementary Notes

Supported by a grant from the US DOT, University Transportation Centers Program

16. Abstract

In several states, bridge deck delamination of reinforced concrete bridge decks built with partial depth precast concrete panels and cast-in-place concrete has been observed. The partial depth precast concrete panels are typically prestressed. Recently, one such failure was observed in Utah. There is a need to develop strengthening and repair methods to re-laminate the partial depth precast concrete panel and cast-in-place concrete deck, ensure composite behavior through mechanical connections, or strengthen the panel such that bridge deck delamination does not pose a safety risk. The goal of the study was to develop numerical models to predict the response of structurally delaminated concrete decks and the response of strengthened decks.

Five retrofit methods were developed to strengthen the deck panels as follows: (1) uni-directional carbon fiber reinforced polymer composite strips bonded to the bottom of the precast section, (2) proprietary mechanical shear anchors connecting the cast-in-place concrete and precast section, (3) high modulus epoxy injection between the cast-in-place and precast sections, (4) nonproprietary shear anchors connecting the cast-in-place and precast sections, and (5) epoxy injection with proprietary shear anchors. Numerical models were developed for three cases to corroborate the laboratory testing: (1) a delaminated deck panel with no retrofit, (2) a nonproprietary shear anchor retrofit, and (3) an epoxy injection retrofit. Similar to laboratory testing, the numerical model concluded that the epoxy injection increases deck panel stiffness, significantly creating a more composite behavior.

17. Key Word	18. Distribution Statement
bridge decks, delamination, precast concrete, predictive models, reinforced concrete bridges, simulation, strengthening (maintenance)	Public distribution

19. Security Classif. (of this report)	20. Security Classif. (of this page)	21. No. of Pages	22. Price
Unclassified	Unclassified	36	n/a

Form DOT F 1700.7 (8-72) Reproduction of completed page authorized

Numerical Simulation of Strengthening of Bridge Decks Built with Partial Depth Precast Concrete Deck Panels

Chris P. Pantelides
Professor

Dylan Briggs
Graduate Student

Department of Civil and Environmental Engineering

The University of Utah

July 2024

Acknowledgments

The authors acknowledge the financial support provided by the Mountain-Plains Consortium (MPC) under project MPC-670.

Disclaimer

The contents of this report reflect the views of the authors, who are responsible for the facts and the accuracy of the information presented. This document is disseminated under the sponsorship of the Utah Department of Transportation, in the interest of information exchange. The Utah state government assumes no liability for the contents or use thereof.

ABSTRACT

In several states, bridge deck delamination of reinforced concrete bridge decks built with partial depth precast concrete panels and cast-in-place concrete has been observed. The partial depth precast concrete panels are typically prestressed. Recently, one such failure was observed in Utah. There is a need to develop strengthening and repair methods to re-laminate the partial depth precast concrete panel and cast-in-place concrete deck, ensure composite behavior through mechanical connections, or strengthen the panel such that bridge deck delamination does not pose a safety risk. The goal of the study was to develop numerical models to predict the response of structurally delaminated concrete decks and the response of strengthened decks.

Five retrofit methods were developed to strengthen the deck panels as follows: (1) uni-directional carbon fiber reinforced polymer composite strips bonded to the bottom of the precast section, (2) proprietary mechanical shear anchors connecting the cast-in-place concrete and precast section, (3) high modulus epoxy injection between the cast-in-place and precast sections, (4) nonproprietary shear anchors connecting the cast-in-place and precast sections, and (5) epoxy injection with proprietary shear anchors. Numerical models were developed for three cases to corroborate the laboratory testing: (1) a delaminated deck panel with no retrofit, (2) a nonproprietary shear anchor retrofit, and (3) an epoxy injection retrofit. Similar to laboratory testing, the numerical model concluded that the epoxy injection increases deck panel stiffness, significantly creating a more composite behavior.

TABLE OF CONTENTS

LIST OF FIGURES

LIST OF TABLES

EXECUTIVE SUMMARY

The primary objectives of this project include: (a) forensic analysis of composite deck samples made with a partial depth precast concrete panels and cast-in-place concrete from the I-15 800 South Bridge, (b) replication of non-composite specimens for testing, (c) destructive testing of retrofitted non-composite deck specimens, and (d) recommended solutions for the repair of bridges affected by debonding of the cast-in-place concrete section from the precast section without impacting traffic.

This report presents the results of the project during which seven full-scale experiments were carried out. The first series of five experiments used bridge deck specimens built in the laboratory, where the precast section was located at the bottom of the deck and was reinforced with prestressing cables in the span direction.

The five retrofit methods were as follows: (1) uni-directional carbon fiber reinforced polymer composite strips bonded to the bottom of the precast section, (2) proprietary mechanical shear anchors connecting the cast-in-place and precast section, (3) high modulus epoxy injection between the cast-in-place and precast sections, (4) nonproprietary shear anchors connecting the cast-in-place and precast sections, and (5) epoxy injection with proprietary shear anchors.

The project's second phase evaluated the performance of two salvaged specimens obtained from the I-15 800 South Bridge. The first salvaged specimen was tested without any retrofit solution, and the second was retrofitted using the epoxy injection method.

Numerical models were developed for three cases to corroborate the laboratory testing: a delaminated deck panel with no retrofit, a nonproprietary shear anchor retrofit, and an epoxy injection retrofit. Similar to laboratory testing, the numerical model concluded that the epoxy injection increases deck panel stiffness significantly, creating a more composite behavior.

After all the testing and analysis, the research team recommends that the epoxy injection retrofit method is the most effective for similarly constructed bridge deck panels affected by this type of debonding behavior.

LIST OF ACRONYMS

CDP	Concrete damage plasticity
HOV	High-occupancy vehicle
LVDT	Linear variable differential transformer
UDOT	Utah Department of Transportation

1. INTRODUCTION

The I-15 over 800 South Bridge in Salt Lake City, Utah, experienced an unexpected blow-through, requiring an emergency closure and repair, on March 24, 2019, as shown in Figure 1.1. After inspection, it was determined that other sections of the deck were in danger of a similar failure. The likely cause of failure was delamination and deterioration of the interface between the cast-in-place and precast sections. The Utah Department of Transportation (UDOT) developed a repair plan, which consisted of removing complete deck sections and replacing the damaged concrete with a rapid-hardening hydraulic cement concrete mix. Three lanes were closed over the 800 South Bridge, and the bridge was re-opened on March 25, 2019. Although this is a viable repair method, it significantly impacts traffic and is a high-cost repair method.

Figure 1.1 Blow-through of deck panel at I-15 and 800 South Bridge (credit: UDOT)

2. DESIGN AND CONSTRUCTION OF TEST SPECIMENS

It was important for the research team to successfully replicate the behavior of the 800 South Bridge in a controlled laboratory setting. The design of the test specimens involved taking measurements from salvaged panels provided by UDOT and technical drawings from other similar bridge construction projects. Forterra Structural Precast supplied the precast panels; a schematic drawing of those panels can be found in Figure 2.1. The cast-in-place section of the composite deck system was constructed by the research team at the University of Utah Structural Engineering Laboratory.

The test specimens were constructed according to the drawings developed during the forensic study of the 800 South Bridge salvaged panels. To prevent the concrete from properly adhering to the precast panel, vegetable oil was applied to the partial depth precast concrete panel surface. The application of vegetable oil serves to create an upper bound for testing (worst-case scenario). The precast panels provided by Forterra were 8 ft x 8 ft in plan dimension. Before the panels were tested, they were cut into 4 ft x 8 ft specimens. Additional information regarding the precast panel is provided in Table 2.1. The cast-in-place portion contained concrete with a 28-day compressive strength of 3,700 psi. Additional compressive strength tests were performed on panel test days with an average compressive strength of 6,500 psi.

Table 2.1 Precast deck panel specifications

Precast Panel Specifications		
f'c	6,000	psi
f'ci	4,500	psi
fpu	270,000	psi
Fi	17.2	Kip
Ff	14.3	Kip

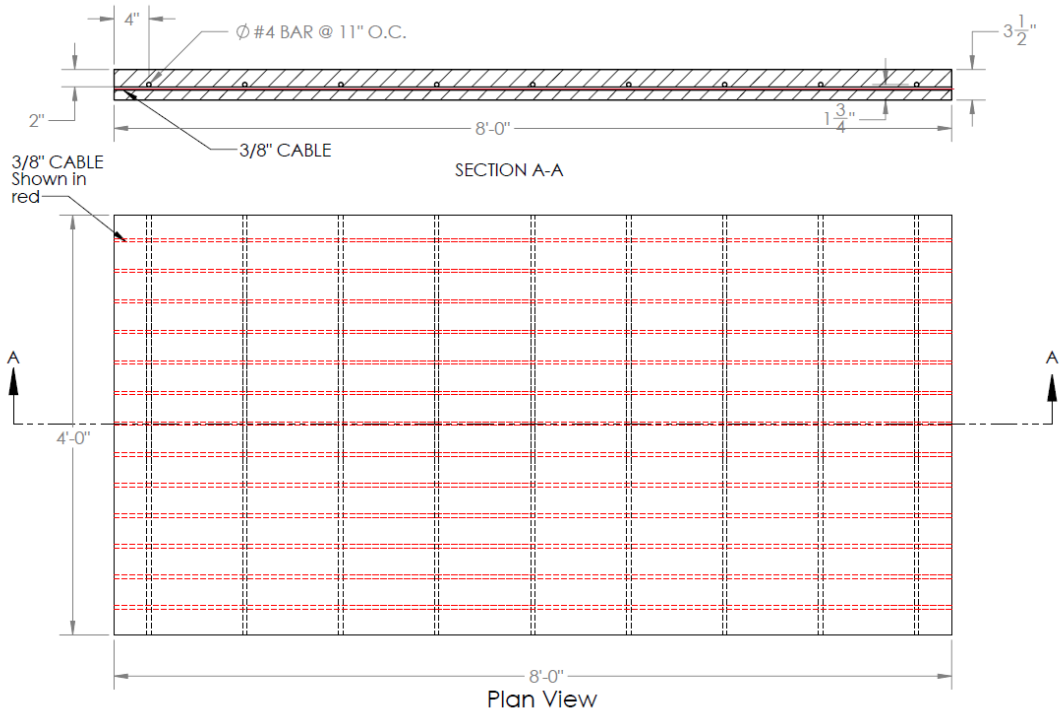

Figure 2.1 Precast deck panel schematic drawing

2.1 Epoxy Injection Retrofit

Epoxy injection has been used successfully as a structural repair option for many years. The theory behind this method of retrofit is to effectively fill the space between the cast-in-place concrete section and precast concrete section of the panels with a high modulus two-part epoxy and permanently bond the two surfaces, preventing separation and forcing the two sections to behave compositely. This method of retrofit also prevents the intrusion of water and other contaminants.

To prepare the panel for epoxy injection, it was necessary to determine the extent that the epoxy could spread between the cast-in-place and precast sections. A simple test was performed using a flat granite slab and 8.5 fluid ounces of water, the volume of one epoxy tube. Water was chosen for the test because the epoxy used has a similar viscosity to that of water. The water was slowly poured over the granite surface and the distribution of the liquid was recorded, as shown in Figure 2.2. The distribution of liquid determines how many injection ports would need to be prepared. With the information obtained from the dispersion test, it was determined that eight injection sites would allow the epoxy to permeate between the cast-in-place and precast sections of the panel.

Eight 1.0 in. diameter holes were drilled into the top of the deck panel and cleared of debris, and the one-way injection ports were installed according to the manufacturer's specifications. A schematic drawing in Figure 2.3 illustrates the port spacing relative to the test panel plan view. Note that the retrofit was performed from the top surface of the cast-in-place portion of the deck, the street surface. This was done for testing purposes only and should not be attempted in the field. Performing the retrofit from the surface allows for the epoxy to fill the void more efficiently between the panels. The epoxy was injected until it was observed exiting from the void between panel sections.

Figure 2.2 Liquid dispersion test

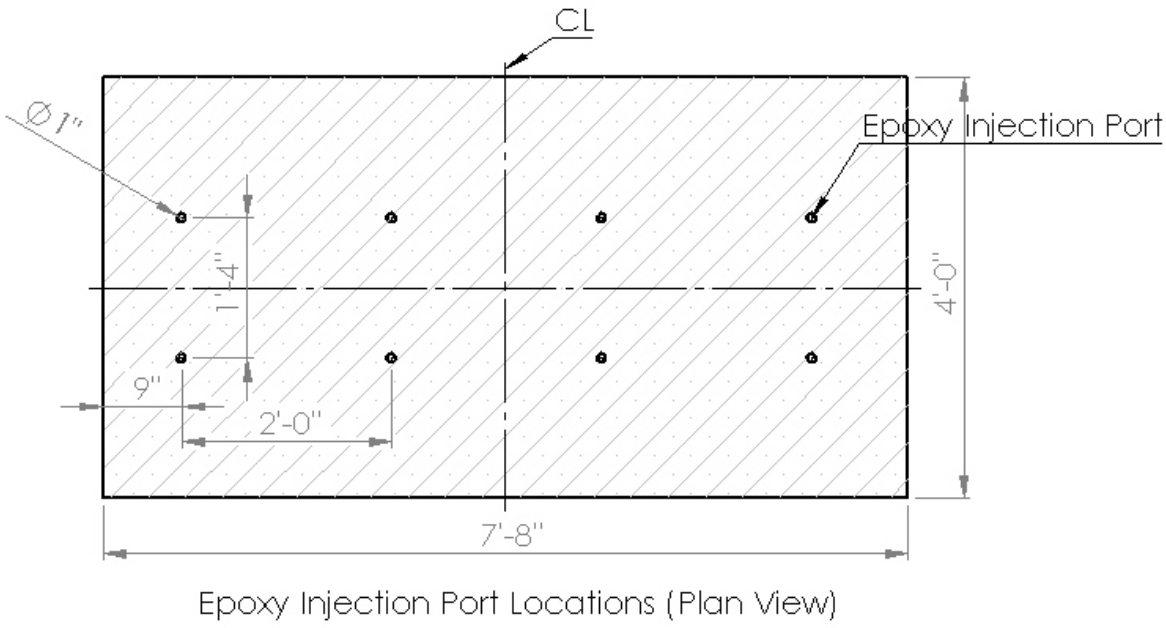

Figure 2.3 Schematic diagram of epoxy injection port spacing (plan view)

2.2 Nonproprietary Shear Anchor Retrofit

Threaded rods with a minimum yield strength of 105 ksi and a zinc corrosion-resistant coating were used as mechanical shear anchors. The anchors were installed according to the schematic drawing shown in Figure 2.4. A nonproprietary anchor is shown in Figure 2.5 before installation. To improve the performance of these anchors, they were offset 12 in. from the centerline. To achieve the required horizontal shear capacity of the composite panel, eight anchors were required. The anchors measured 6 in. in length and were embedded until they were flush with the precast panel.

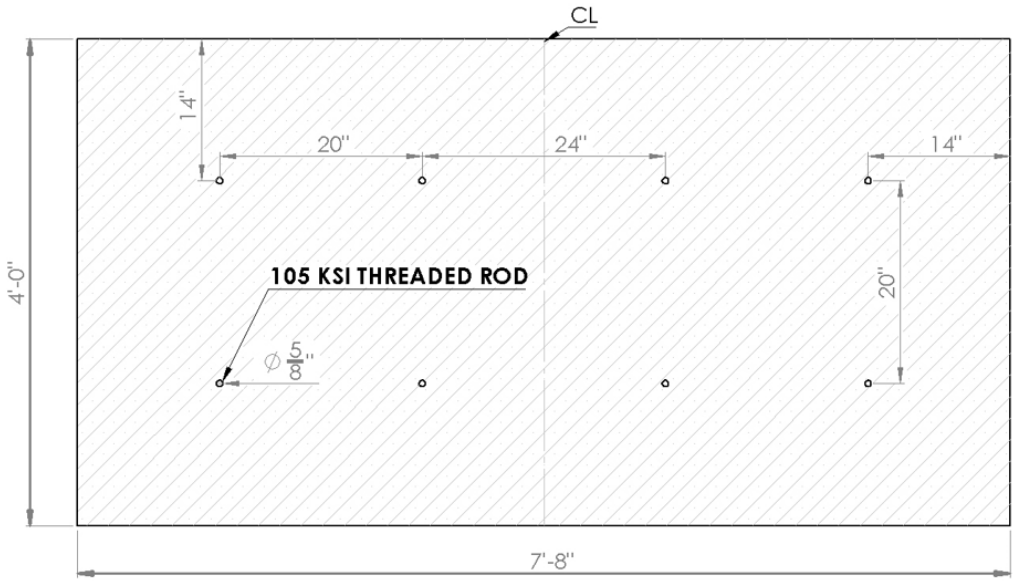

Figure 2.4 Nonproprietary shear anchor placement

Figure 2.5 Nonproprietary shear anchor prior to installation

3. TEST SETUP AND RESULTS

3.1 Test setup

All testing was performed at the University of Utah Structural Laboratory. The testing was carried out using a test frame with the ability to resist 500 kip in each direction. A 120-kip servo-controlled hydraulic actuator was positioned vertically to apply a displacement-controlled loading protocol at the center of each panel.

The panels were positioned on the top of two steel rollers to allow for smooth movement and rotation of each panel as it responded to the imposed displacement. Figure 3.1 shows a schematic drawing of the panel and its position on the test fixture. For each test, the clear span was kept at a consistent 87-in. length. The load was applied at the center of each panel through a 1-in.-thick steel plate with the dimensions shown in Figure 3.2.

Three linear variable differential transducers (LVDT) were used to capture the linear movement of the test specimens at strategic locations on the panel as it responded to the applied loading. Two LVDTs (north and south LVDT) were placed at the north and south extremes of the specimen to measure the separation of the cast-in-place section from the precast section, as shown in Figure 3.3. Another LVDT (midspan LVDT) was placed on the underside of the panel at midspan to capture the total deformation. The applied force was recorded using a calibrated load cell between the hydraulic actuator and the test panel.

A monotonic half-cyclic displacement-controlled force was applied to each of the test specimens. Figure 3.4 shows the displacement applied at each interval using the initial load protocol. The displacement increased at a rate of 0.2-in./sec with a 30-sec dwell between each loading cycle; at 1.2 in. displacement, the loading rate was increased to 0.4-in./sec with the same 30-sec dwell between cycles.

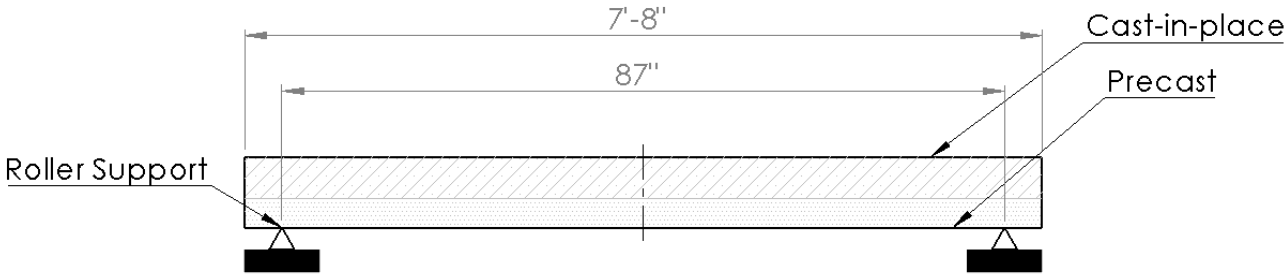

Figure 3.1 Test frame schematic drawing (profile view)

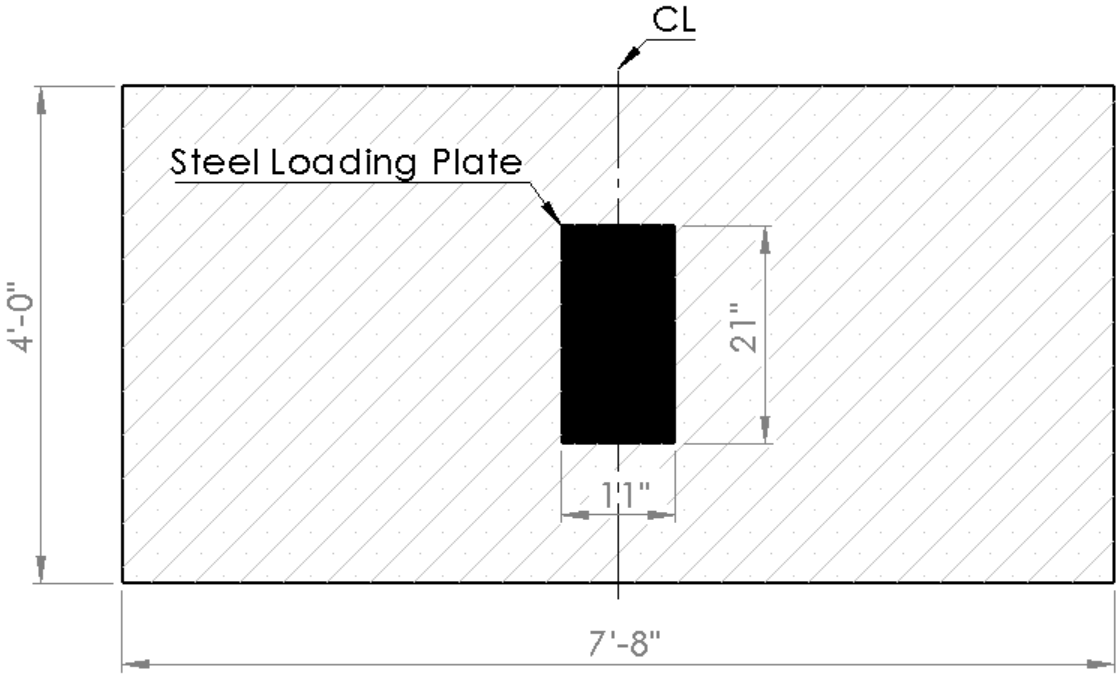

Figure 3.2 Schematic drawing of concrete panel with loading plate (plan view)

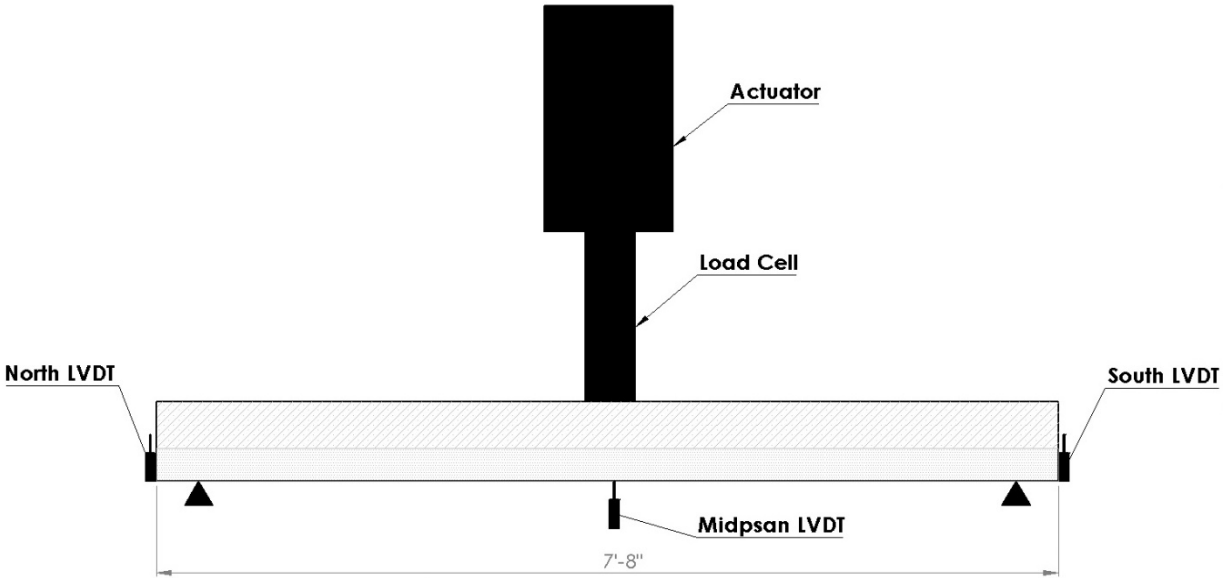

Figure 3.3 Schematic drawing of the instrument locations (profile view)

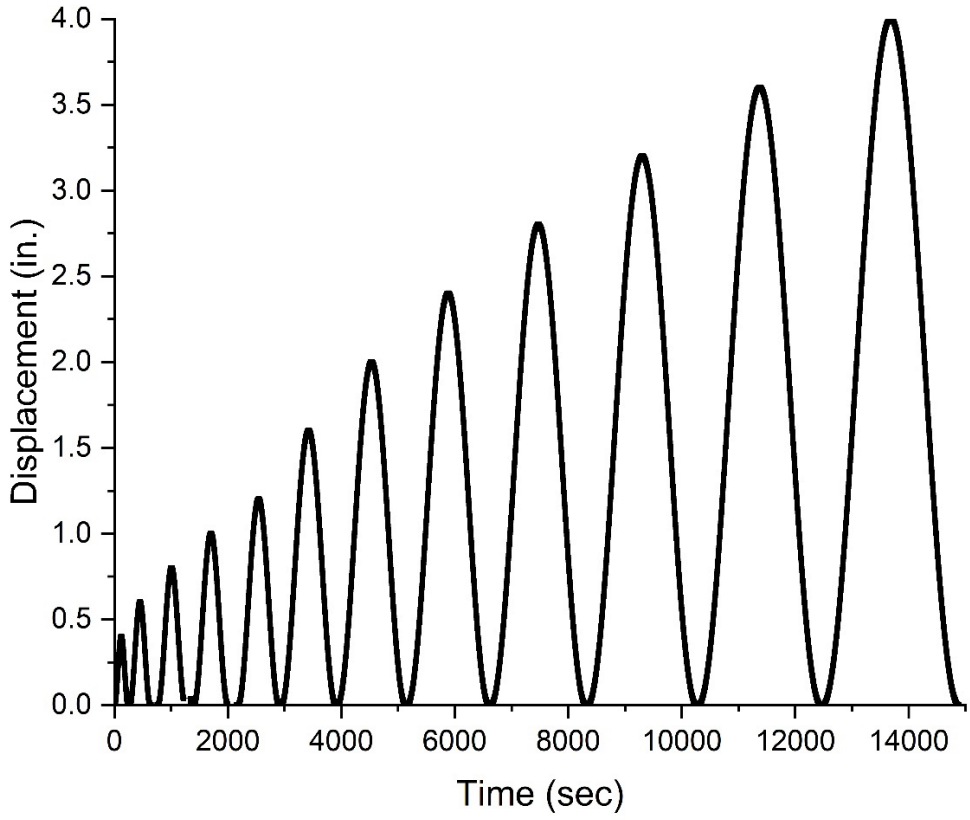

Figure 3.4 Loading protocol

3.2 Test Results

Test 1 – Panel with No Retrofit

To generate a baseline for comparison, a delaminated panel without any retrofit was tested as the control specimen. Note that all measurements made using the LVDTs do not include this initial delamination.

The unmodified deck panel behaved in a manner consistent with a non-composite specimen. The precast and cast-in-place sections of the panel visually appeared to be acting independently of one another. At the end of the sixth displacement cycle (1.2 in.) the delamination became immediately visible. Figure 3.5 shows the separation of the two panels at the southwest corner after the 1.2-in. displacement cycle.

The most critical information captured from each test cycle is shown in Figure 3.6. This graph displays the specimen displacement at the north and south extremes as recorded by the LVDTs. It is evident in this graph that as the applied displacement increases, the panel is unable to fully recover, and the gap continues to grow. Not only does the delamination increase the deflection but the deflection becomes permanent, and the specimen's strength is ultimately compromised. The hysteresis curves of the entire loading protocol have been included along with the point of delamination in Figure 3.7. This figure shows with a red circle the point where delamination became visible (1.2 in.).

The LVDT plot in Figure 3.6 indicates that internal delamination started at an applied displacement of 0.5 in. due to the reduction in stiffness at that point in time. It is also at this point that small cracks began forming on the underside of the precast panel.

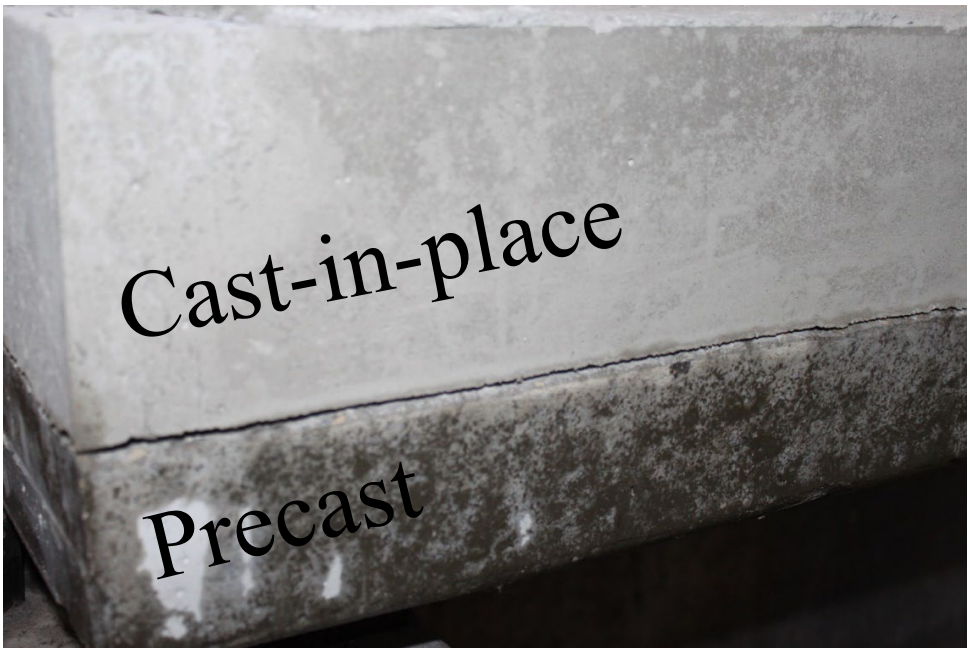

Figure 3.5 Unmodified test specimen delamination at 1.2 inches of displacement (location: northwest)

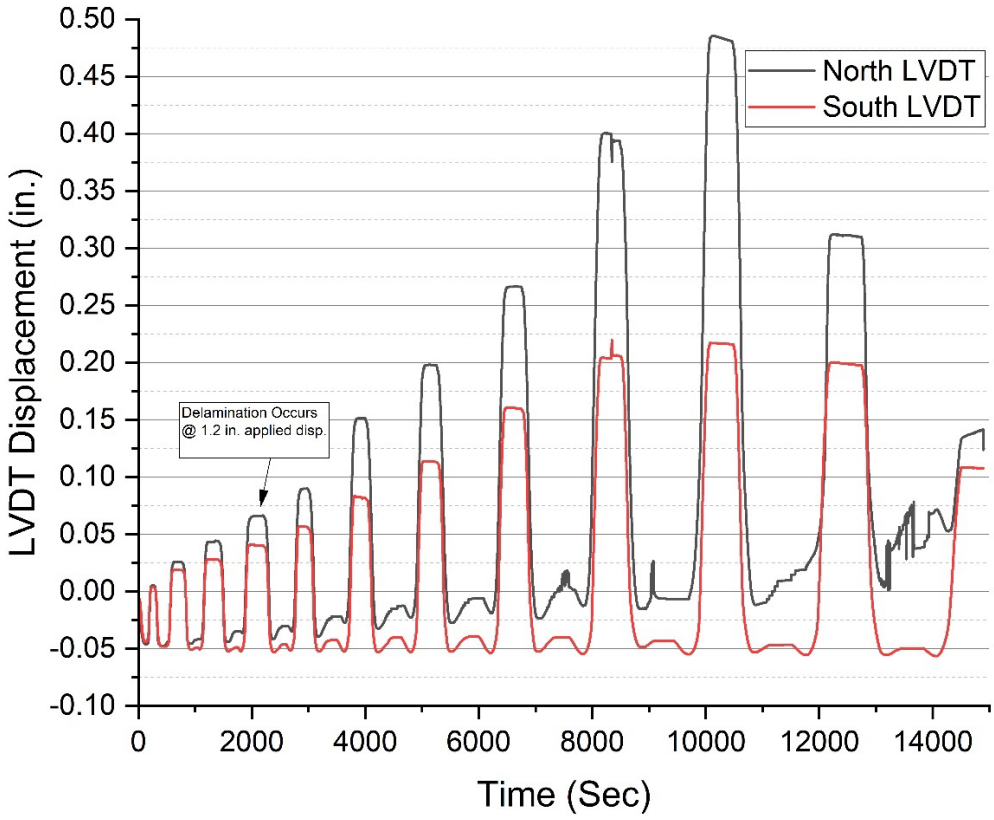

Figure 3.6 Test specimen with no retrofit (control) LVDT displacement at north and south

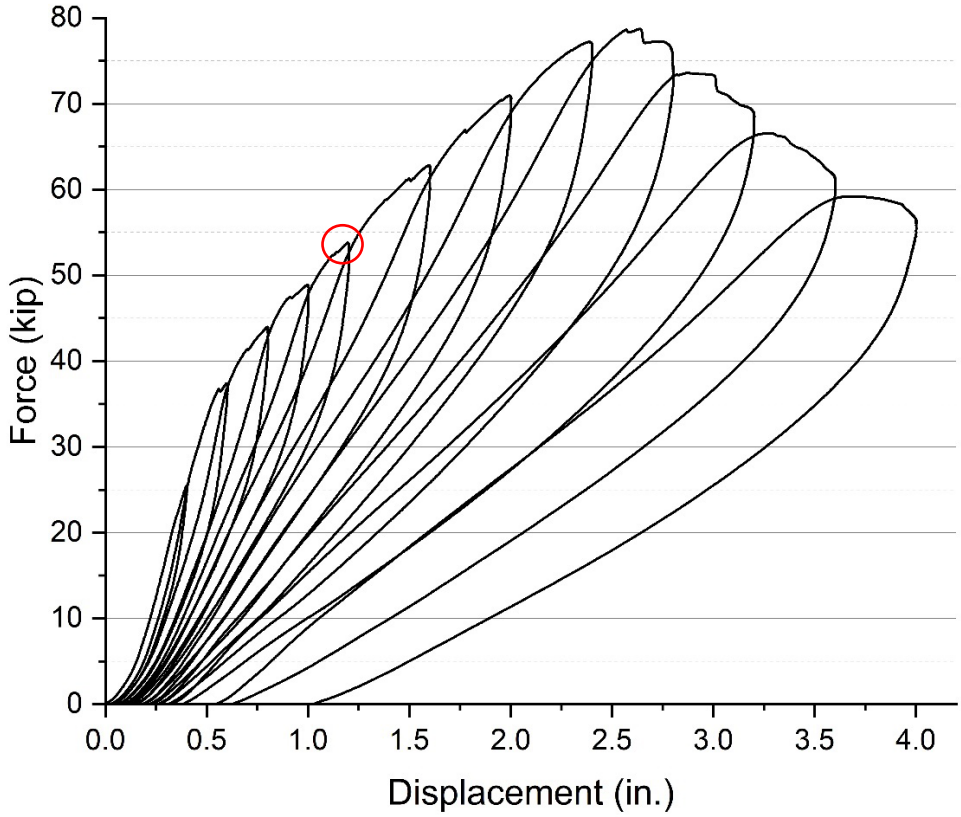

Figure 3.7 Test specimen with no retrofit (control) hysteresis with point of visible delamination circled in red

Test 2 – Panel with Epoxy Injection Retrofit

The deck panel with the epoxy injection retrofit resisted the displacement imposed by the hydraulic actuator until the epoxy bond between the precast section and cast-in-place section of the panel failed. The epoxy retrofit demonstrated perfectly composite behavior for the first cycle of 0.4-in. Once the epoxy bond had failed, the panel behaved almost identically to the panel without any retrofit. This bond failure occurred at only the north side of the panel while the south end remained completely bonded; this type of failure created a large displacement in the north LVDT, as shown in Figure 3.8. The panel with epoxy bond was able to endure a maximum load of 63 kip before delamination, as indicated in the hysteresis curves of Figure 3.9. The precast and cast-in-place sections of the panel continued to separate after the epoxy bond failure.

Once the test was stopped, the precast and cast-in-place panels were removed and separated to verify the dispersion of the epoxy between the panel sections. Figure 3.10 shows that the epoxy had been able to fill the void between the two panels at each extreme; this image also highlights the difficulty in injecting the epoxy in areas that do not have complete interlayer delamination.

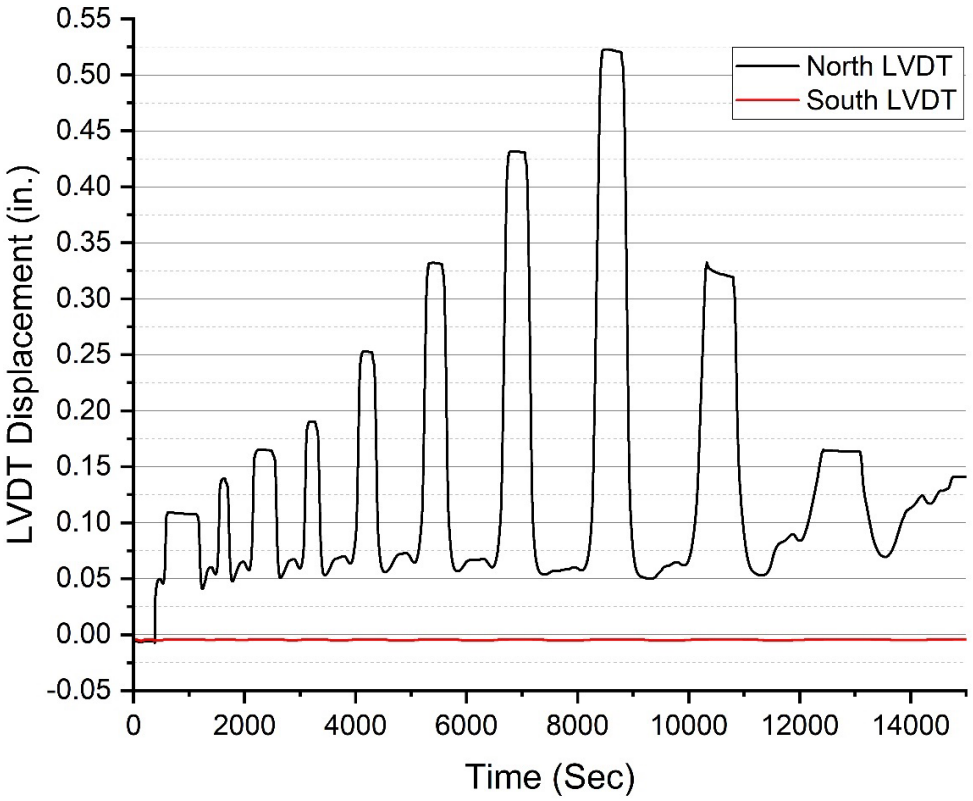

Figure 3.8 Epoxy retrofit panel LVDT displacement at north and south

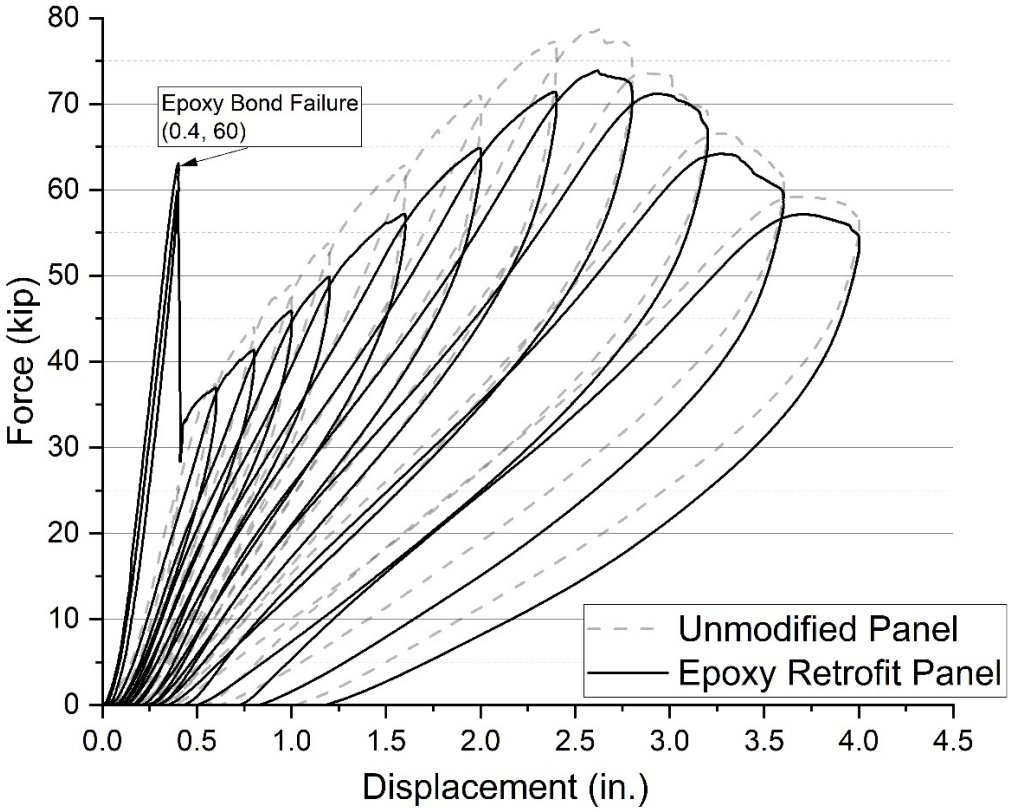

Figure 3.9 Epoxy retrofit panel hysteresis compared to the unmodified panel

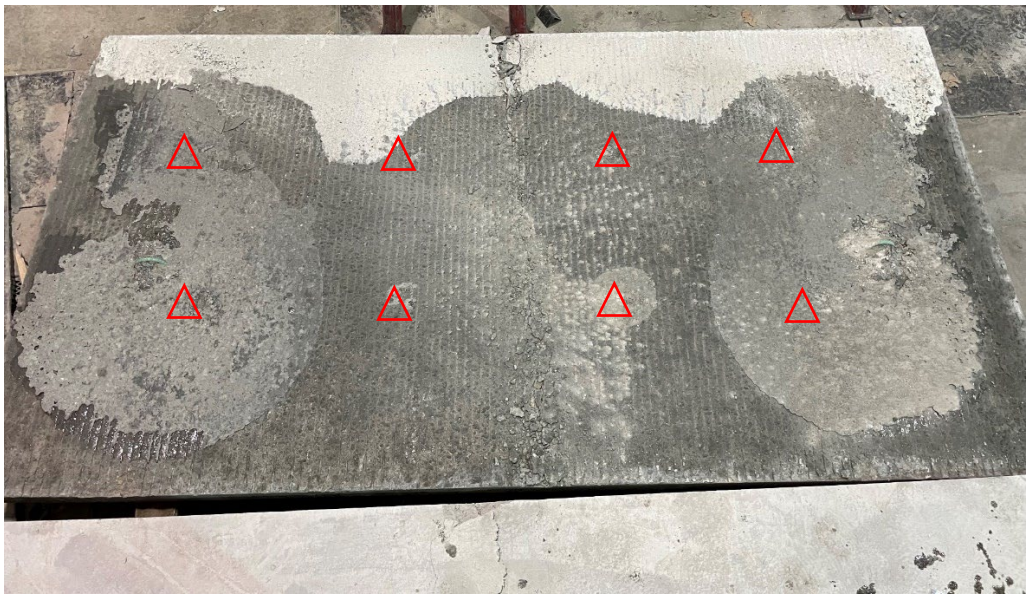

Figure 3.10 Distribution of epoxy after testing on the precast panel surface (Triangles indicate location of the epoxy injection sites)

Test 3 – Nonproprietary Mechanical Shear Anchors

Small flexural cracking began at 1.6 in. of displacement at the mid span of the panel. Even at 2.0 in. of applied displacement, the shear slip at the north and south extremes between the two panels was negligible. After the test, the panel was inverted and evaluated revealing significant cracking along the underside of the panel. No failure of the tendons was observed in the precast panel. The primary failure mode for this specimen was the crushing failure at the top cast-in-place section. Figure 3.11 shows the hysteresis of the panel with nonproprietary anchors.

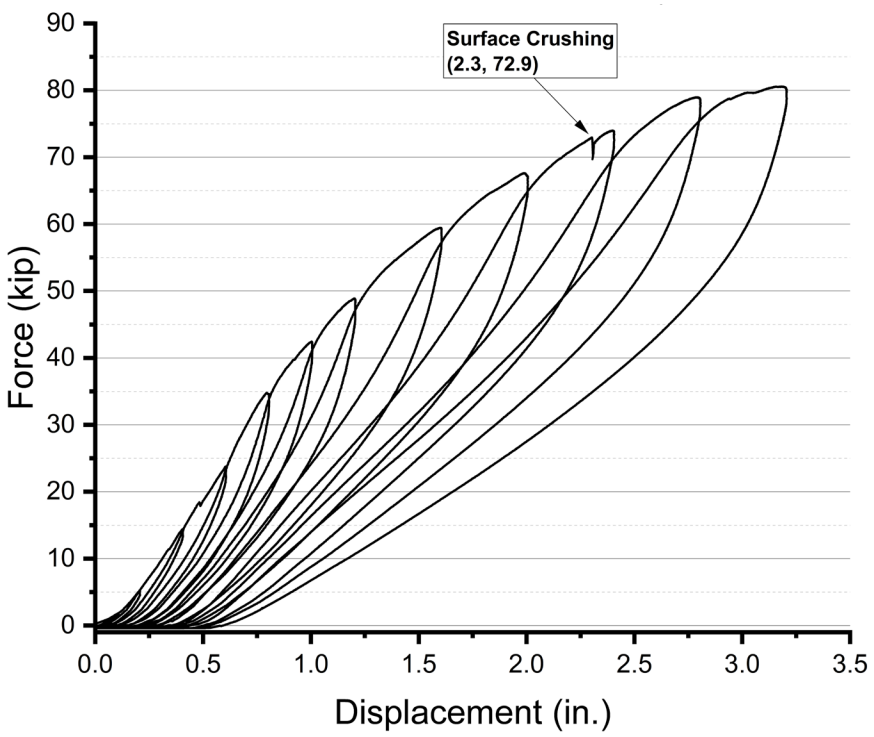

Figure 3.11 Nonproprietary shear anchor hysteresis

4. NUMERICAL MODEL

4.1 Material Model

4.1.1 Concrete Damage Plasticity Model

A reliable technique for modeling the nonlinearity of concrete in structural analysis is the concrete damage plasticity (CDP) model, which is integrated into ABAQUS (Smith 2019). It accurately illustrates the relationship between stress and strain in concrete under various loading conditions by combining material plasticity and isotropic damage elasticity. This model is beneficial for modeling the response of concrete structures under different load conditions because it captures significant phenomena such as strain-softening and tension-stiffening. The CDP model can simulate both tensile cracking and compressive crushing as a failure mode (Lee and Fenves 1998). The overall reliability of structural analysis has been improved by the successful prediction of the failure processes and structural response of concrete elements using the CDP model in numerical analysis. The CDP model for this analysis was generated for concrete with a compressive strength of 8.0 ksi and used for modeling. The precast panel was aged and was assumed to have a compressive strength of 8.0 ksi; the compressive strength of the cast-in-place section was approximately equal to 6.5 ksi, but the finite element model (FEM) required a higher compressive strength to replicate the experimental results. Figure 4.1 shows the material properties of the CDP material used in the FEM modeling of the bridge decks. Table 4.1 shows the plasticity parameters used in the ABAQUS model to simulate the actual behavior of concrete.

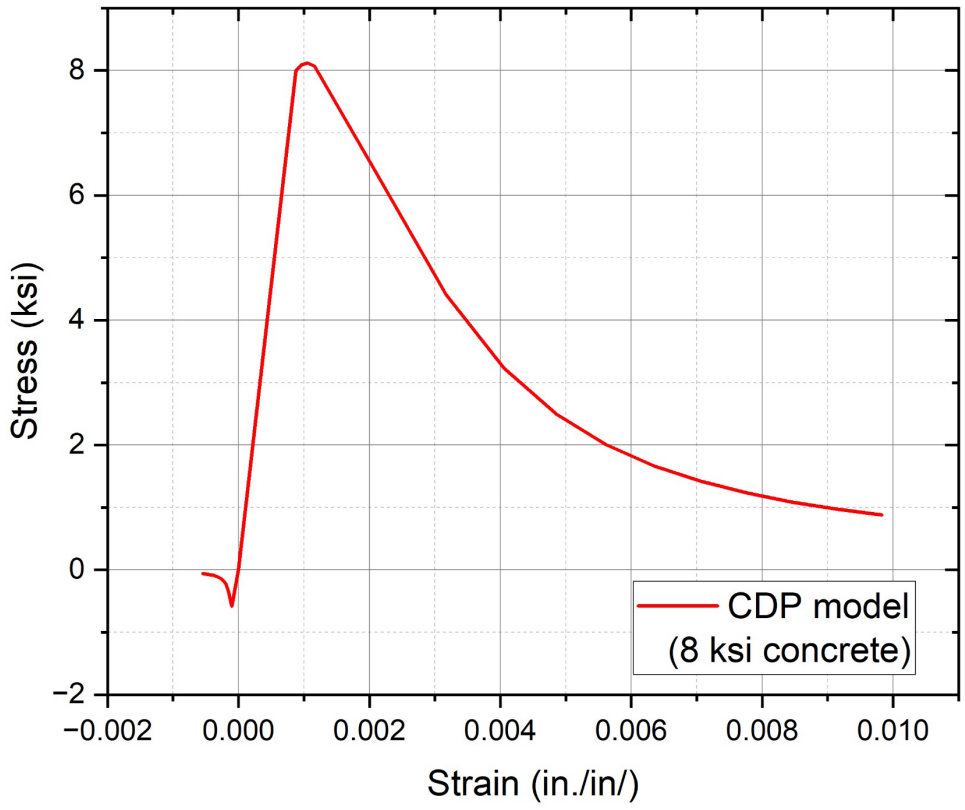

Figure 4.1 Concrete damage plasticity model material properties

Table 4.1 CDP material properties

Dilation angle	Eccentricity	Fb0/fc0	K
35	0.1	1.16	0.667

4.1.2 Steel Reinforcement and Prestressed Tendon Material Properties

In the experimental study ASTM A615, Grade 60 steel reinforcing bars were used; standard properties of these bars were used for modeling them with finite elements. The reinforcing bars were represented as truss elements incorporating steel reinforcement properties. The specific reinforcing bars had a yield strength of 68 ksi and an ultimate strength of 99 ksi. The stress-strain curve for the reinforcing bars used in the finite element model is shown in Figure 4.2(a). This curve shows the typical behavior of mild steel reinforcing bars under the applied loading conditions, serving as a fundamental component in the accurate representation of their response within the finite element model. Prestressed tendons are used in the long axis of the precast concrete section. The finite element model in ABAQUS incorporates the physical nonlinear characteristics of the 7-wire strand tendons in the numerical model, and an initial predefined stress is applied to replicate the initial prestress in the tendons. The material properties of the prestressed tendons used in the finite element model are shown in Figure 4.2(b).

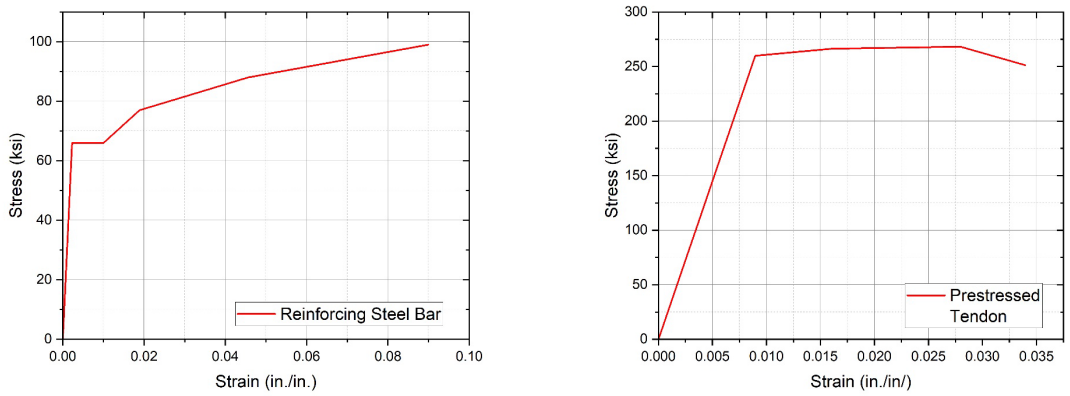

(a) (b)

Figure 4.2 Steel reinforcement material properties: (a) steel reinforcing bars; (b) prestressed tendons

4.2 Model Layout

Two different deck panels were modeled in ABAQUS. The CDP material properties are included in the FEM model to represent both tensile and compressive failure within the concrete; both panel sections are modeled as a C3D8R solid brick element type. A 0.5-in.-thick steel plate was used to distribute the load; this loading plate was tied together with the concrete surface on the cast-in-place section. A reference point was created and coupled to the top surface of the loading plate simulating the load distribution of the actuator during the experiment. The loading plate was modeled as a solid C3D8R brick element. D-shaped elastic supports were modeled as supports to simulate the simply supported connection during the experiment and modeled as solid C3D8R brick elements. Boundary conditions are applied to represent the experimental setup. The D-shaped steel support was modeled as an elastic material, and only general friction with a frictional coefficient of 0.45 in the tangential direction and hard contact in the normal direction was used to simulate the interaction between the supports and the bottom slab surface. Figure 4.3 shows the experimental setup with the supports and actuator load application in the loading plate using a reference point.

The reinforcing bars are modeled as wired truss elements present in ABAQUS. Linear T3D2 material with material properties of the longitudinal reinforcing bars were used to model the reinforcing bars. The longitudinal reinforcing bars have the same total area as the bars in the experiment. Longitudinal reinforcing bars are embedded in the concrete surface of the top and bottom sections of the panel to represent the behavior of the reinforcing bars inside the concrete, as shown in Figure 4.4(a) and 4.4(b). Similarly, the 7-wire strand prestressed tendons were modeled as linear T3D2 wired truss elements and were embedded in the bottom slab, as shown in Figure 4.4(b). The physical nonlinear properties of the tendons are integrated into the numerical model, and an initial predefined stress is applied using a predefined stress function in ABAQUS to emulate the initial prestress in the tendons. The material properties of the prestressed tendons used in the finite element model are presented in Figure 4.2(b). In the FEM model, a vertical displacement of 1.0 in. was applied; a tabular function was used to define the amplitude and loading rate for the monotonic load. The actuator was limited to vertical movement while movement in all other directions was restricted. The load applied to the reference point of the ABAQUS model was constrained to only allow vertical movement, simulating the actual experimental setup. The explicit analysis solver technique available in ABAQUS was used for the nonlinear dynamic analysis.

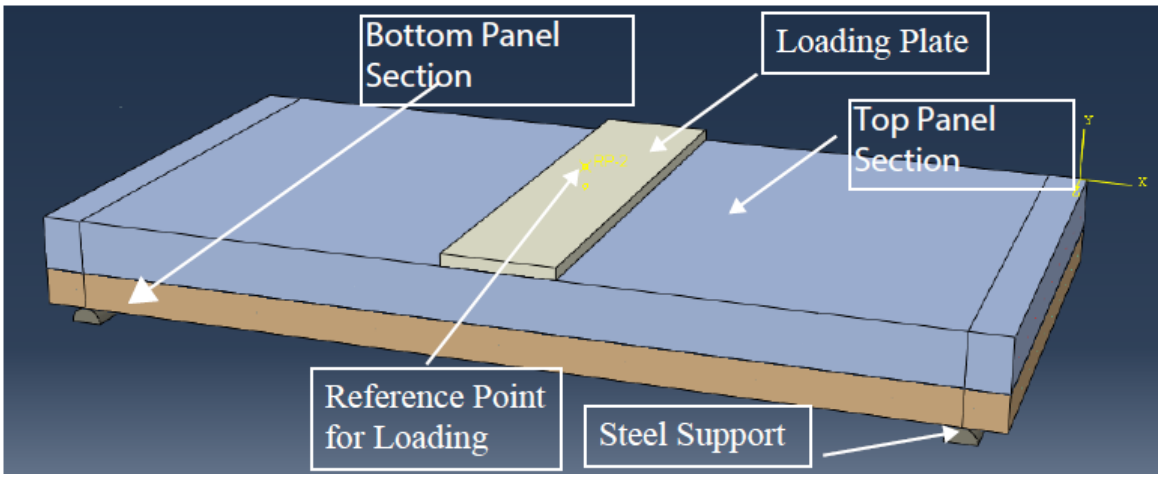

Figure 4.3 FEM model elevation schematic showing supports and loading interface

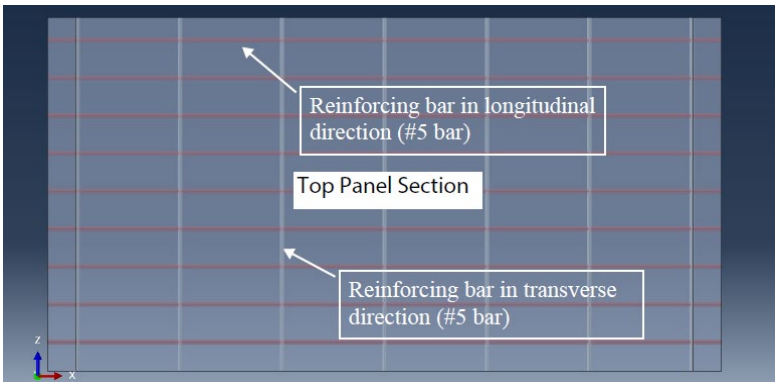

(a)

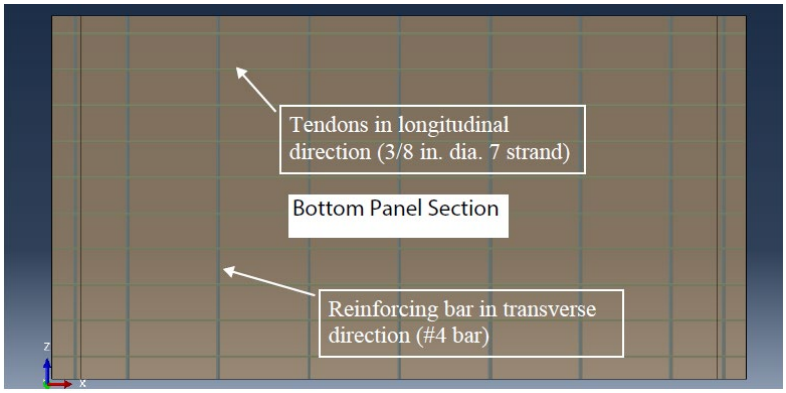

(b)

Figure 4.4 Reinforcing details: (a) top panel section; (b) bottom panel section

4.3 Numerical Model – Test Panel with No Retrofit

A numerical model was created for the specimen without any retrofit. A vertical load was imposed at the reference point, and both panel sections were meshed with a 1-in. mesh size for all the solid and wire elements. A mesh sensitivity analysis was conducted for various mesh sizes, and the optimal mesh size, which produced nearly identical results, was selected as the final mesh size for the FEM model. The material properties and model layout detailed in the preceding section were used. As no contact improvement measures were implemented, only frictional contact existed between the two slab surfaces. The interaction between the slab surfaces was simulated using a general friction parameter with a tangential friction coefficient of 0.45 and hard contact in the normal direction. This behavior was replicated in ABAQUS to represent the contact between the two slabs. The 3D view of the meshed structure is shown in Figure 4.5. The elevation of the structure and arrangement of the steel reinforcement in the concrete slab is shown in Figure 4.6. Figure 4.7 shows the deflected shape of the structure along with the Von-Mises stress. The deflected shape closely resembles that of the experimental result.

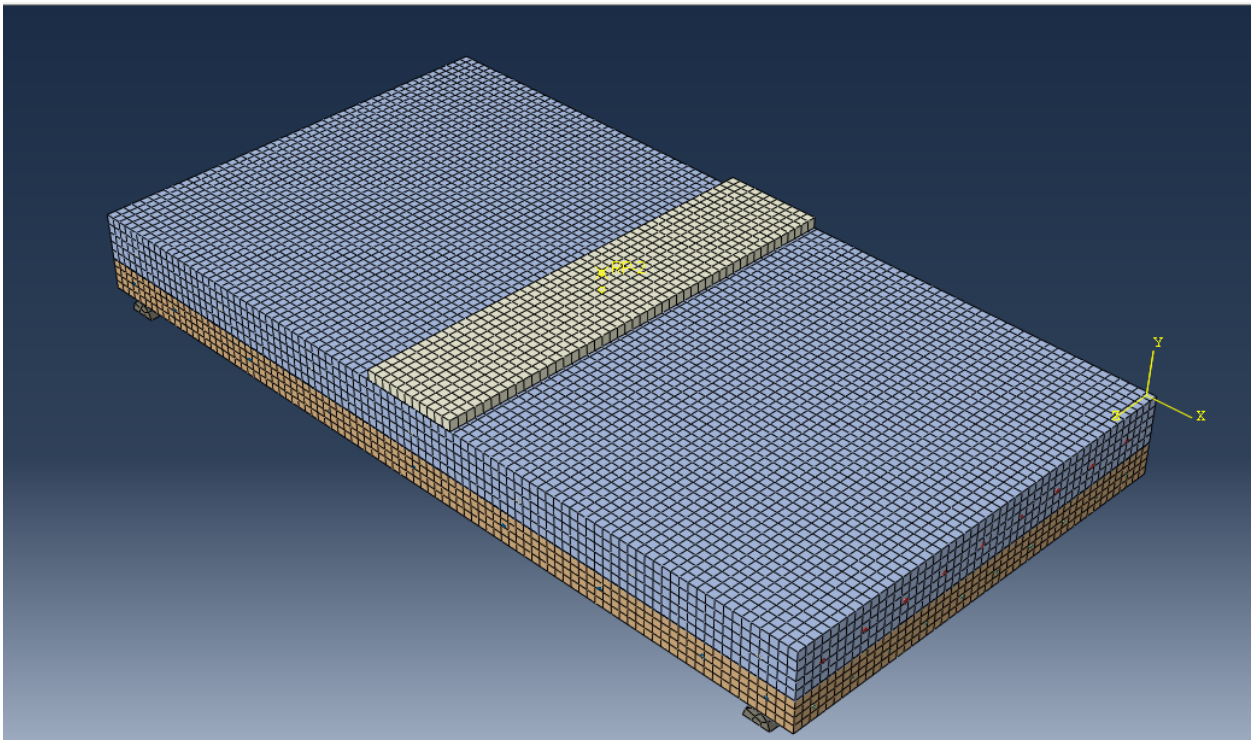

Figure 4.5 Meshed structure of test specimen with no retrofit

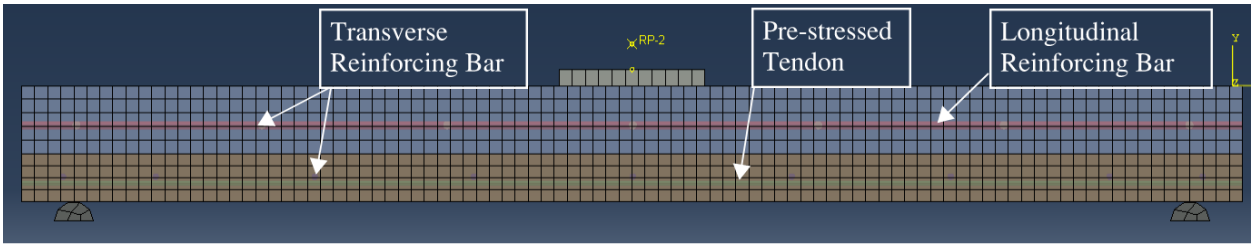

(a)

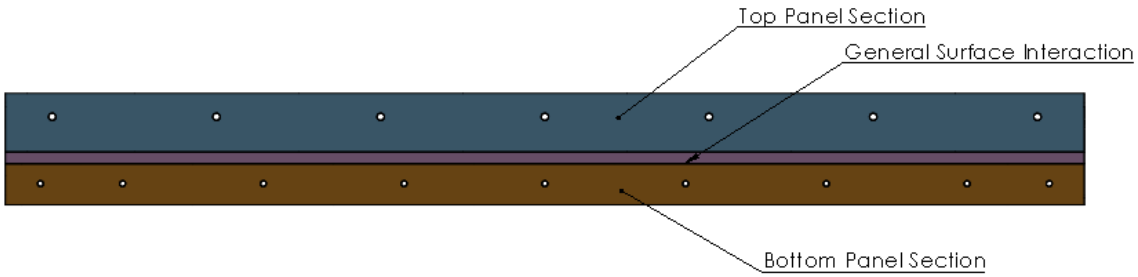

(b)

Figure 4.6 (a) meshed structure showing elevation and reinforcing bars; and (b) schematic diagram showing general surface interaction for surface friction

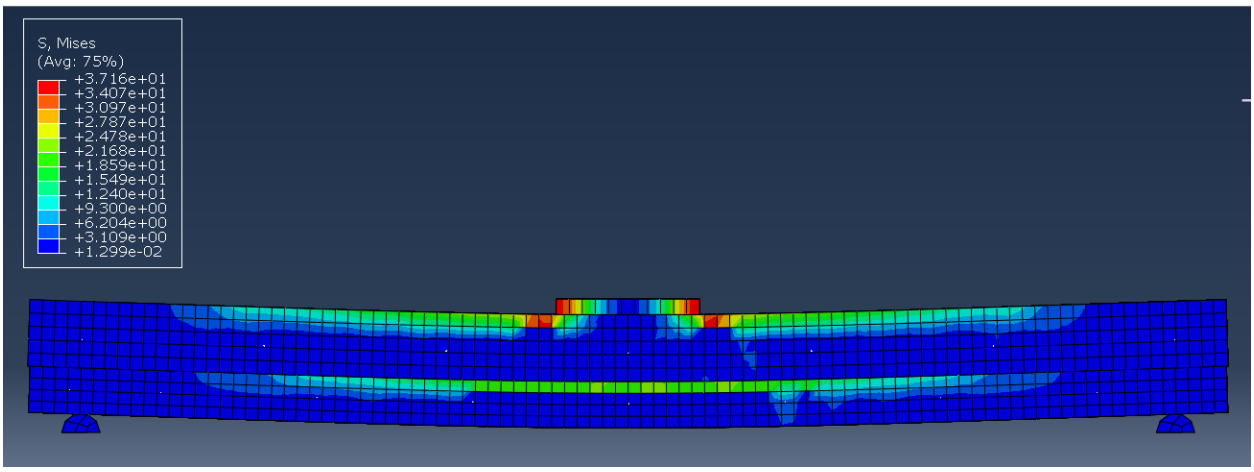

Figure 4.7 Deflected shape with Von-Mises stress (MPa) (1-in. displacement)

The force-deformation response for the specimen was computed, and a monotonic plot was generated, which was then compared against the force versus displacement envelope obtained from the experimental study. Figure 4.8 shows the comparison of force versus displacement curve from the experiment and the ABAQUS model. The results indicate that the FEM model effectively predicts the response of the deck panel, including the delamination effect; it was able to predict the peak load within a 2.0% margin of error and exhibited nearly identical initial stiffness to the experimental study. Minor variations were observed due to geometrical irregularities and construction defects, which were idealized in the FEM model.

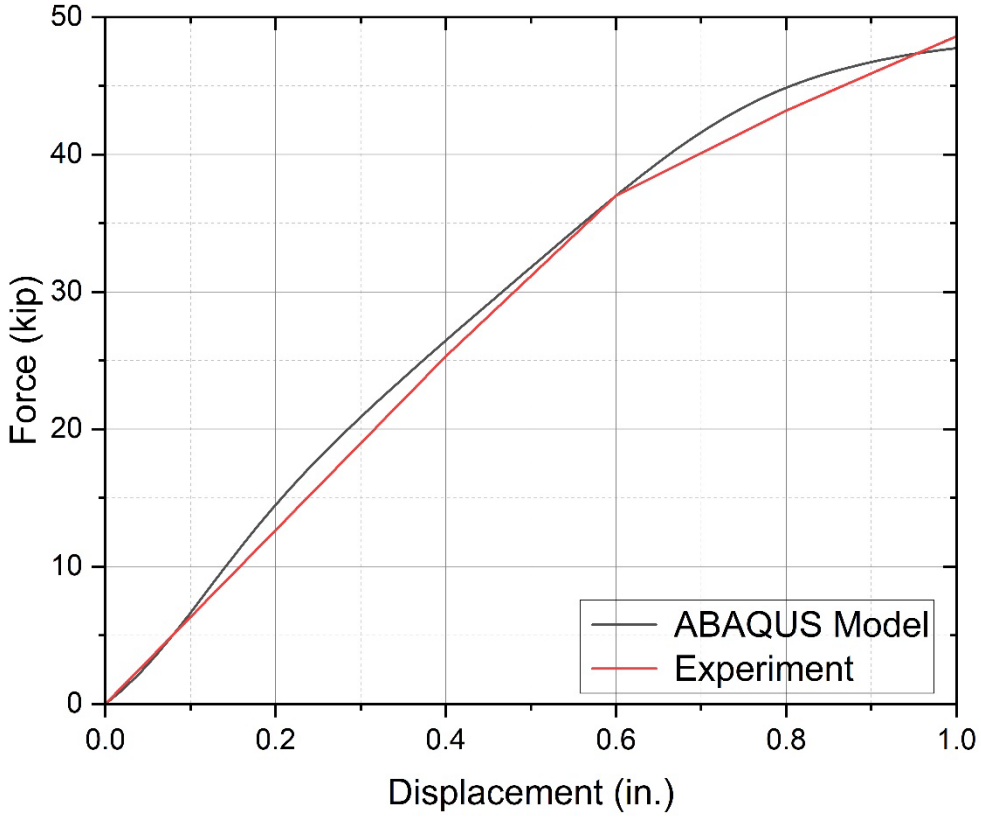

Figure 4.8 Force vs. displacement of test specimen with no retrofit

4.4 Numerical Model – Epoxy Injection Retrofit

A numerical model was created for the test panels that used the epoxy injection method. The base layout of the numerical model had similar mesh size and loading rate as used in the specimen without any retrofit. To model the behavior of epoxy in ABAQUS, the cohesive modeling technique can be used to define the epoxy adhesive layer. This involves using a surface contact property to define cohesive material properties of the epoxy. The cohesive surface contact represents an adhesive material with a finite thickness. ABAQUS provides the necessary modeling capabilities for this purpose, allowing for the accurate representation of the epoxy behavior within the simulation; it allows the user to input fracture energy of the epoxy and stiffness in the normal, tangential, and shear direction. This approach is commonly employed to simulate delamination and adhesion in various material systems (Alfano and Crisfield 2001). For the FEM model with cohesive element, fracture energy, which included damage evolution properties of the cohesive element representing epoxy, was used; the stiffness in the normal direction was assumed as 70 ksi, and in both tangential directions the stiffness was assumed as 22 ksi. The 3D model was similar to the model without any retrofit by changing the general surface frictional contact with the properties of cohesive contact. Figure 4.9 shows the cohesive surface interaction applied between the two bridge deck panel sections to represent the contact created by the epoxy injection. Figure 4.10 shows the deflected shape of the structure along with the Von-Mises stress. Figure 4.11 shows the damage initiation in the surface contact element and the damaged epoxy when 1.0 in. vertical displacement is applied on the bridge deck panel.

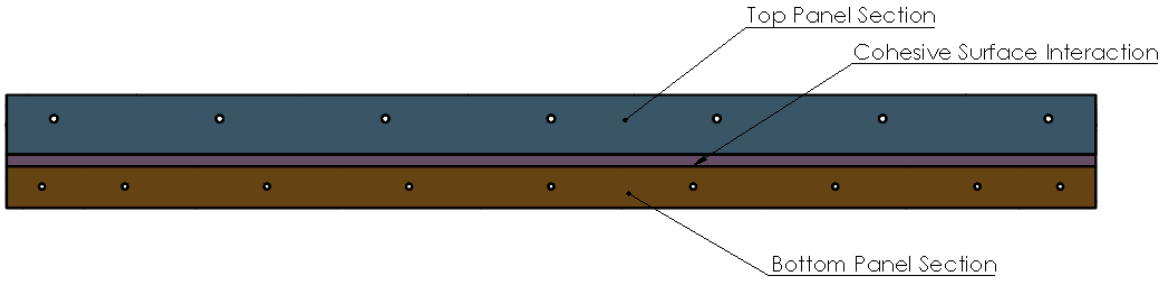

Figure 4.9 Cohesive surface interaction between cast-in-place and precast sections

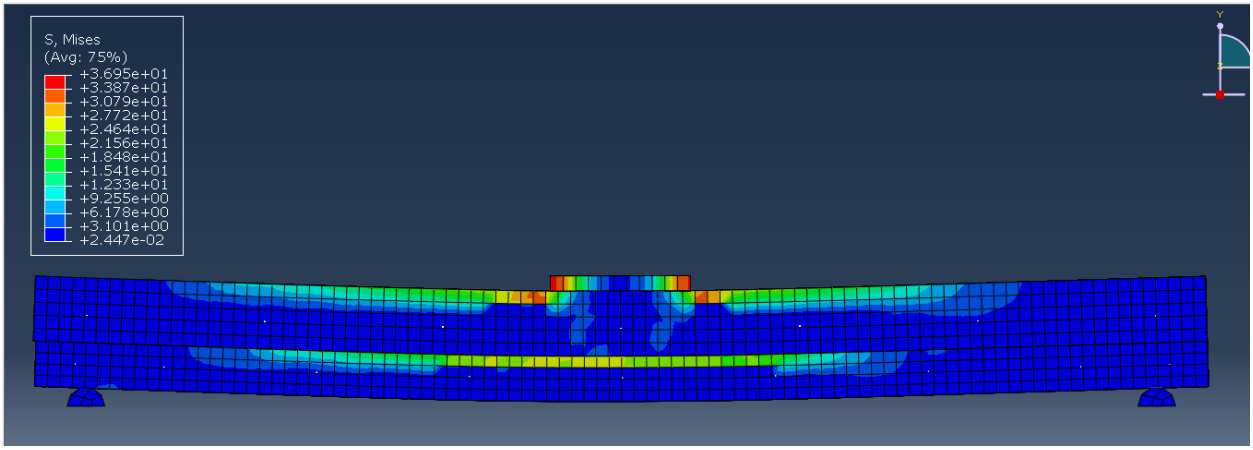

Figure 4.10 Deflected shape of epoxy retrofit specimen with Von-Mises stress (MPa) (1-in. displacement)

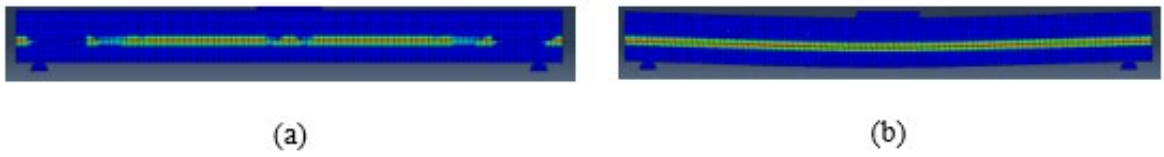

Figure 4.11 Cohesive contact: (a) damage initiation; and (b) damage at vertical deflection of 1.0 in.

The deformed shape closely aligns with that of the experiment. The force-deformation response for the specimen was calculated, and a monotonic load versus displacement plot was generated, which was then compared to the envelope curve from the experimental study. The results indicate that the FEM model effectively predicts the panel response, including damage initiation in the epoxy, lateral load rise due to the inclusion of epoxy, and the delamination effect. The FEM model was able to predict the peak load and initial stiffness, which were almost identical to the experimental study. Minor variations were observed due to geometrical irregularities and constructional defects, which were idealized in the FEM model. Figure 4.12 illustrates the comparison of the force-displacement curve from the experiment and the ABAQUS model.

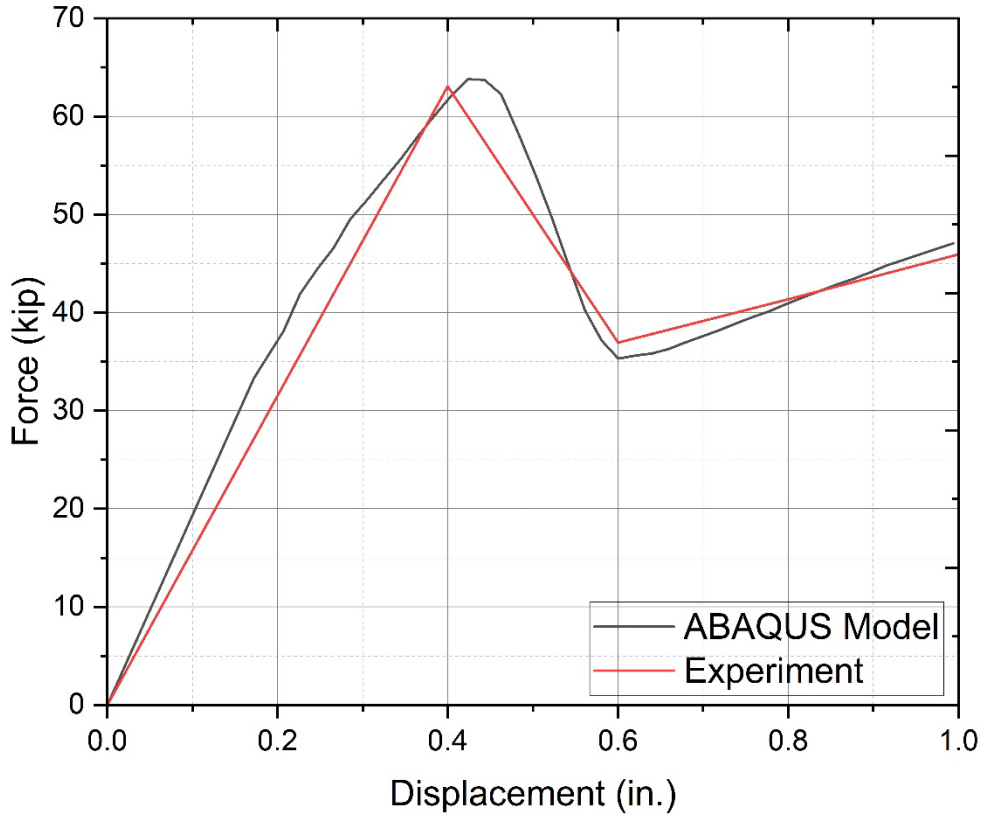

Figure 4.12 Force vs. displacement curve: epoxy injection retrofit

4.5 Numerical Model – Nonproprietary Shear Anchors

The numerical model was created for the specimen with nonproprietary shear anchors as a retrofit element. Anchors were modeled as elastic elements with a modulus of elasticity equivalent to 29,000 ksi since no yielding of the anchors was observed during the experiment. Since the anchors were drilled and bonded together with the epoxy, all anchors were embedded in both the cast-in-place and precast sections of the panel. Anchors were modeled as linear wired T3D2 truss elements. The interaction between the panel section surfaces was simulated using a general surface contact friction parameter with a tangential friction coefficient of 0.45 and hard contact in the normal direction. This behavior was replicated in ABAQUS to represent the contact between the two sections. The 3D view of the meshed structure and bottom panel section showing embedded anchors is shown in Figure 4.13. The elevation of the structure and the arrangement of the rebar and prestressed tendons in the concrete panel are shown in Figure 4.14. Figure 4.15 shows the deflected shape of the structure along with the Von-Mises stress. The deflected shape closely resembles that of the experimental result.

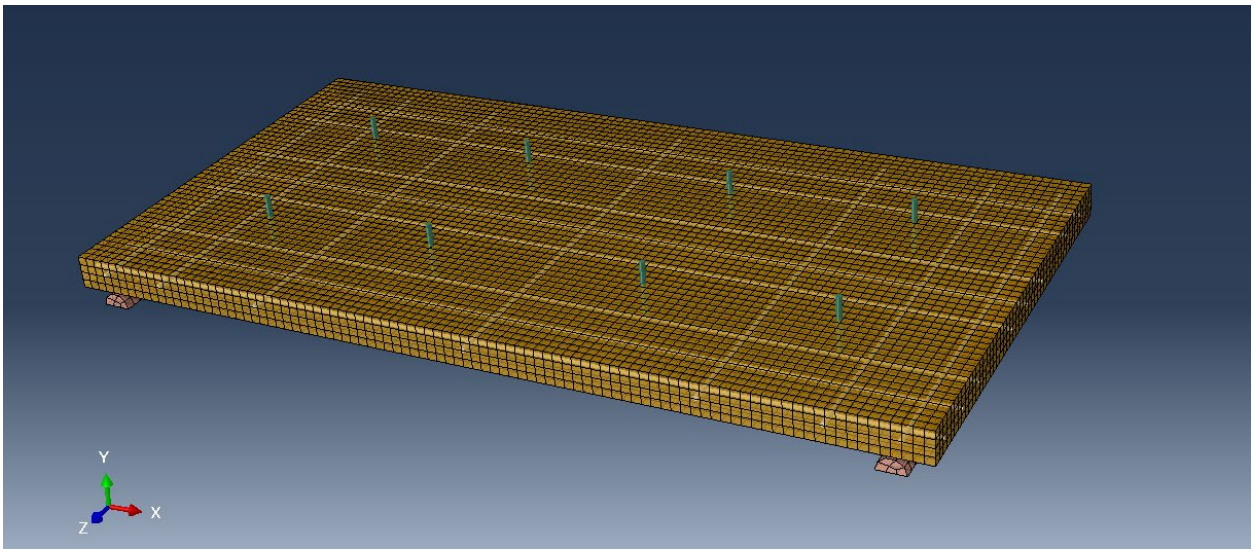

Figure 4.13 Meshed structure of precast panel

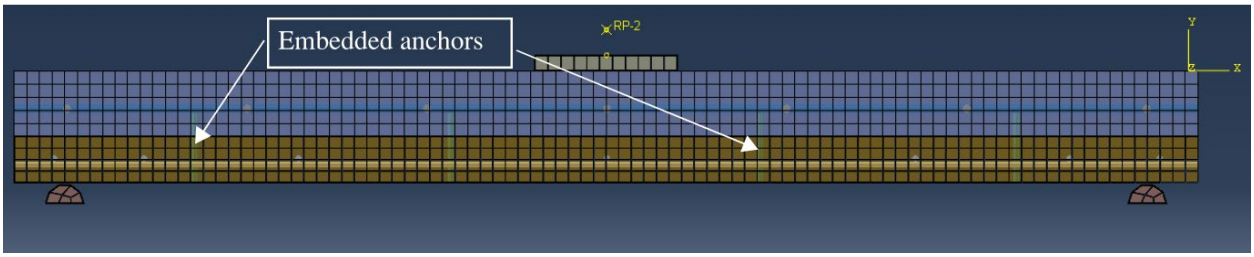

Figure 4.14 Meshed structure highlighting embedded anchors

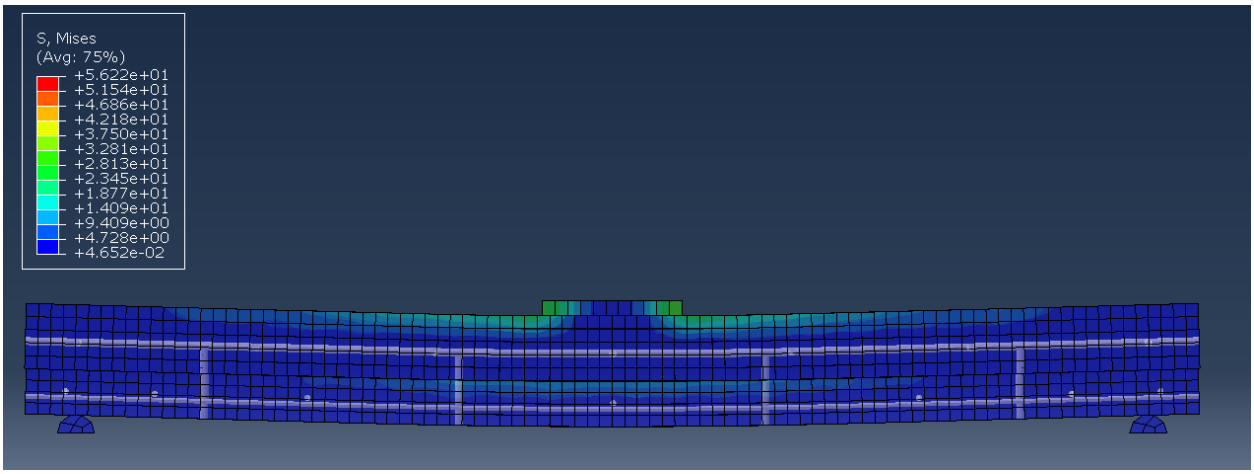

Figure 4.15 Deflected shape with Von-Mises stress (MPa) (1.0 in. displacement)

The force-deformation response for the specimen was computed, and a monotonic plot was generated, which was compared against the envelope curve obtained from the experiment. Figure 4.16 compares the force-displacement curve from the experiment with the ABAQUS model. The results indicate that the FEM model effectively predicts the response of the deck, including the delamination effect. It could predict the peak and initial stiffness to be almost identical to the experiment. Minor variations were observed due to geometrical irregularities and constructional defects, which were idealized in the FEM model.

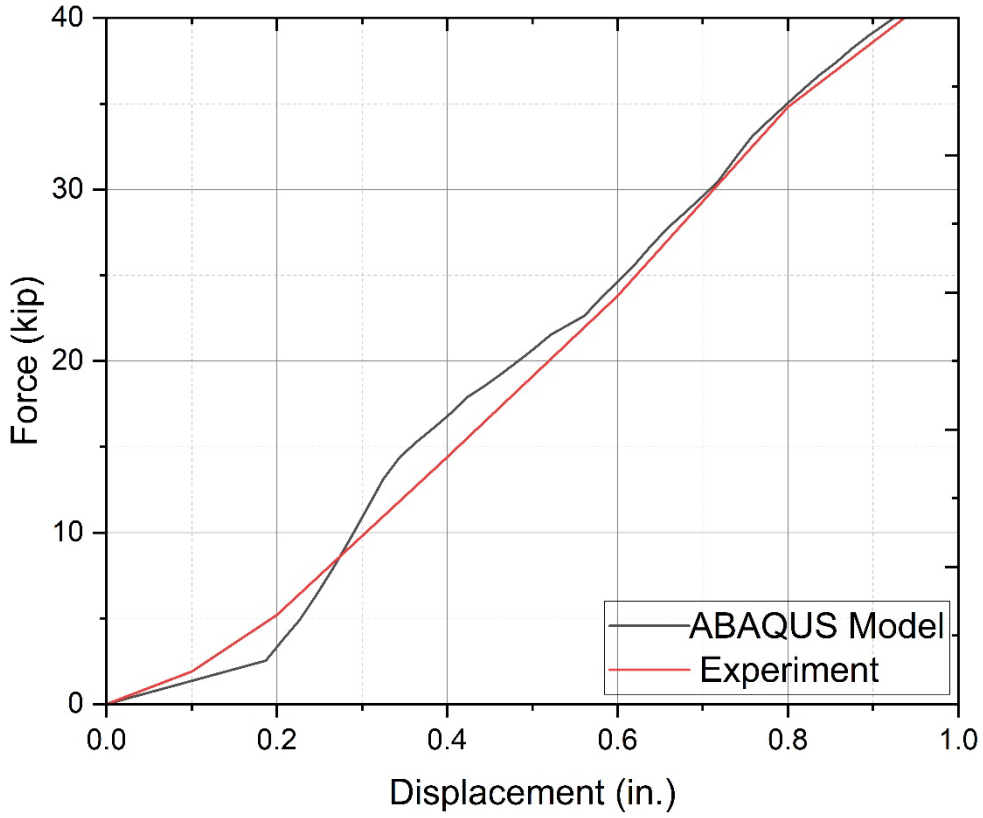

Figure 4.16 Force vs. displacement curve: nonproprietary anchor retrofit

5. CONCLUSIONS

The study presents a comprehensive analysis regarding the non-composite behavior of concrete bridge decks using partial depth precast concrete and cast-in-place structural components. This report presents findings from two different methods of retrofitting conventional bridge decks with prestressing cables running parallel to the span between girders. The two retrofit methods would not impact traffic at the surface level. These methods include:

- High modulus epoxy injection
- Nonproprietary shear anchors

The testing contained both a quantitative and qualitative analysis to conclude which method would minimize interlayer delamination and separation of the cast-in-place section from the precast section. The performance of each retrofit method was evaluated using the data obtained from the various instruments on each test specimen and compared against the control specimen.

Computational models were developed to evaluate the bridge deck performance. These models include a test panel with no retrofit, one with epoxy injection retrofit, and one with nonproprietary shear anchors. The deflected shapes closely resemble those of the experimental results for all three cases. Moreover, comparisons of the force-displacement curves from the experiment to the finite element models indicate that they effectively predict the experimental response of the deck, including the delamination effect, as well as the peak and initial stiffness. The potential impact to the road surface during retrofitting was also evaluated. The test results indicate that both retrofit methods showed improved performance compared with the test specimen without any retrofit.

Bridge decks are not anticipated to see more than 1.0 in. of deflection in service. Additionally, bridge decks are not expected to perform within the plastic range and are designed to behave elastically. The research team recommends that the epoxy injection method of retrofit should be used to retrofit bridge decks of this type. Not only does this method of retrofit encourage composite action of the panels, it also improves the overall strength. The method also decreases the possibility of water intrusion within the delaminated portion of the panels. For future construction of partial depth bridge decks, all precast panels are to be washed, degreased, and dried before the cast-in-place concrete is poured. Where possible, the precast deck should be free of any snow or ice prior to casting concrete.

6. REFERENCES

Alfano, G., and Crisfield, M.A. (2021). “Finite element interface models for the delamination analysis of laminated composites: mechanical and computational issues.” *International Journal for Numerical Methods in Engineering* 50, 1701–1736.

Lee, J., and Fenves, G.L. (1998). “Plastic damage model for cyclic loading of concrete structures.” *Journal of Engineering Mechanics* 124:892-900.

Smith, M. (2019). *ABAQUS/Standard User’s Manual, Version 6.9*. Dassault Systèmes Simulia Corp.